ORIGINAL RESEARCH (AR) DOI: 10.4274/jems.2025.83792

Journal of ETA Maritime Science

Assessment of Biofouling and Antifouling Performance on Glass Fiber Reinforced Polymer (GFRP) Hulls

Refik Özyurt, Mehmet Cihan

Ordu University Fatsa Faculty of Marine Sciences, Department of Naval Architecture and Marine Engineering, Ordu, Türkiye

Abstract

This study investigates the early-stage biofouling development on recreational vessel hulls represented with Glass Fiber Reinforced Polymer (GFRP) test panels under natural marine environments. GFRP test panels, both coated with a commercial antifouling product and uncoated, were immersed in the Black Sea for 10 weeks and monitored for biofouling accumulation using Naval Ship's Technical Manual (NSTM) fouling ratings. Environmental parameters such as seawater temperature, salinity, and weather conditions were also recorded throughout the immersion. Results showed that uncoated panels reached advanced slime accumulation (NSTM rating 20) within approximately 30-35 days and began developing grass filaments (NSTM rating 30) by day 35-40, the coated panels delayed advanced slime formation until nearly day 70. Fouling progression was then effectively modelled using a logistic growth function, enabling prediction of fouling severity over time. The model supports biofouling prediction under different operational profiles and emphasises the importance of antifouling coatings in mitigating hull degradation. Additional correlations between fouling ratings, equivalent sand roughness (k_s), and average coating roughness (Rt_{50}) provide a foundation for assessing hydrodynamic impacts and coating performance in recreational marine applications.

Keywords: Biofouling, GFRP hull, recreational vessels, roughness correlation, antifouling coating efficacy

1. Introduction

Biofouling is the phenomenon of organisms' attachment tendency on man-made surfaces. This phenomenon has consistently become one of the most persistent challenges to overcome in many industries, including shipping [1], aquaculture [2], marine renewable energy [3], and offshore installations [4]. Among the others, biofouling increases hull roughness, altering the ship's hydrodynamic form, resulting in added resistance up to 80% that may lead up to 10.7% slower steaming for a Oliver Hazard Perry class frigate (FFG-7) compared to a foul-free ship hull scenario [5]. Additionally, biofouling maintenance costs reach up to $1 billion over 15 years for a DDG-51 class [6]. What is more, by applying antifouling coatings on crude oil and bulk carriers, 138 t of fuel can be saved and 430 t CO_2 emission release can be prevented per route [7]. Beyond operational and economic burdens, biofouling also facilitates the spread of invasive species, posing ecological threats to marine biodiversity [8].

Several methods exist for preventing biofouling, so that antifouling strategies can be divided into physical, biological and chemical approaches [9]. Biological antifouling strategies typically rely on the secretion of enzymes or natural compounds from organisms that have biofouling deterrents. However, the low stability of the enzyme secretion process, with a lack of practicality in application, is still considered a major problem, making biological antifouling strategies insufficient as feasible antifouling deterrents [10-12]. In contrast, physical antifouling strategies rely on structural and material properties such as the use of acoustics [13], electric or magnetic fields [14], ultraviolet (UV) light [15], and engineered surface topographies [16]. Despite the wide variety of these approaches, many have been developed within recent years and remain at an initial stage of development. As a result, the lack of long-term performance data and cost-effectiveness makes the majority of physical antifouling strategies insufficient. In other words, while physical antifouling strategies are considered promising for

Address for Correspondence: Asst. Prof. Refik Özyurt, Ordu University Fatsa Faculty of Marine Sciences, Department of Naval Architecture and Marine Engineering, Ordu, Türkiye
E-mail: refikozyurt@odu.edu.tr
ORCID iD: orcid.org/0000-0002-9596-6291

Received: 22.06.2025
Last Revision Received: 21.07.2025
Accepted: 22.07.2025
Epub: 23.07.2025

To cite this article: R. Özyurt, and M. Cihan, "Assessment of biofouling and antifouling performance on glass fiber reinforced polymer (GFRP) hulls," *Journal of ETA Maritime Science*, [Epub Ahead of Print]

the future, current studies based on these methods are not yet dependable [17].

Chemical antifouling strategies remain among the most common, feasible, and cost-effective antifouling methods preferred in the maritime industries [18]. From traditional antifouling coatings to modern chemical antifouling coatings, majority of the coating systems function as releasing toxic materials into the marine environment [19], thereby preventing fouler organisms from attaching to surfaces, enabling a foul-free surface [12]. Among the others, two types of antifouling coatings are highly recognised within modern chemical antifouling coatings: self-polishing copolymer (SPC) coatings and foul release (FR) coatings [20].

Foul-release coatings are regarded as the future of the antifouling coatings due to their non-toxic, environmentally friendly mechanisms [21,22]. Buskens et al. [23] conducted a research reviewing foul-release coatings to discuss alternative antifouling coatings for replacing SPC coatings. Additionally, Hu et al. [24] investigated developments of foul-release coatings with a particular focus on high-performance foul-release coatings. That is to say, although there are many studies conducted showing the impacts of biofouling for the vessels coated with the FR coatings [25,26], overall, widespread adoption of FR coatings across maritime sectors remains a question [27], due the relatively higher costs and poor performances for the vessels operating under idle conditions [21].

In contrast with the foul-release coatings, SPC coatings function by releasing toxic biocides into the marine environment. Lagerström et al. [19] investigated SPC antifouling leach and found that slowest leaching rate of copper in marine waters was 1.9 $\mu m/cm^2$ per day. These toxic biocides act as deterrents so that any fouler organism attempting to attach to the coated surface faces with the potential death threat. Due to being one of the earliest methods, this mechanism makes SPC coatings highly effective and economically feasible in the fight against biofouling [12,28,29]. Consequently, numerous studies have been conducted on SPC coatings, clearly demonstrating their effectiveness in the fight against biofouling [30]. However, while only a few early investigations have explored the efficacy of SPC coatings on wooden ships, most of the research has been primarily concentrated on SPC applications involving steel-hulled ships.

Thai et al. [31] conducted nanocomposite antifouling coatings performance on a steel substrate using natural marine water in a laboratory. Falara et al. [32] investigated five commercially available antifouling coatings on naval steel by focusing on antifouling and anticorrosive performances. Zhao et al. [33] attempted to develop an environmentally friendly Cu-bearing stainless steel as an antifouling coating. Zhou et al. [34] developed an antifouling coating for galvanised steel, which is reported to be as a successful antifouling method for preventing certain fouler organisms. Daloğlu et al. [35] investigated a glass-ceramic coating applied to steel substrates, which ended up effectively resisting biofouling. Suleiman et al. [36] investigated the anticorrosion and antifouling performances of biocides embedded in hybrid coatings on mild steel. Soma Raju et al. [37] highlighted sol-gel-based organic and inorganic hybrid coatings for steel. That is to say, existing research concerning marine biofouling has predominantly focused on the challenges associated with commercial vessels constructed with steel.

In contrast, the impact and characteristics of biofouling on recreational vessels, which are primarily fabricated from Glass Fiber Reinforced Polymer (GFRP), have received considerably less extensive investigation. Kadir et al. [38] investigated two coatings with the compounds of polytetrafluoroethylene, polydimethylsiloxane, and polyvinylidene fluoride on GFRP Composite materials through visual observation. In addition to that, Subramanian and Williams [39] demonstrated how banned Tributyltin-modified epoxy polymers for glass fiber reinforced composites are more successful than traditional antifouling coatings. This disparity in research attention represents a significant oversight, particularly given the operational profile of leisure vessels.

Sánchez and Yebra [40] investigated methodologies for marine antifouling coating performance tests, distinguishing between laboratory-based and field-based testing approaches. In their study, a representative pyramid was generated to demonstrate how accurate antifouling performance tests are. Short-term tests are located at the base of this pyramid, which represents the least initial and the least conclusive performance tests. Upon satisfactory outcomes, medium-term tests are conducted, followed by long-term tests and finally, full-scale ship tests are conducted. Therefore, ship tests are the most accurate antifouling coating performance tests. However, that should be noted that the economic viability of such trials is often impractical. Overall, research conducted by Sánchez and Yebra [40] showed that long-term field tests are frequently considered as the most practical and reliable method for evaluating antifouling coating performances. Figure 1 illustrates the efficient antifouling coating design and optimisation workflow.

Moreover, experimental panels submerged for ten weeks are considered representative of the upper range of biofouling accumulation anticipated on commercial vessels maintaining frequent operational schedules [41-43]. Such vessels, often benefiting from advanced anti-fouling systems and regular movement through water, typically experience a

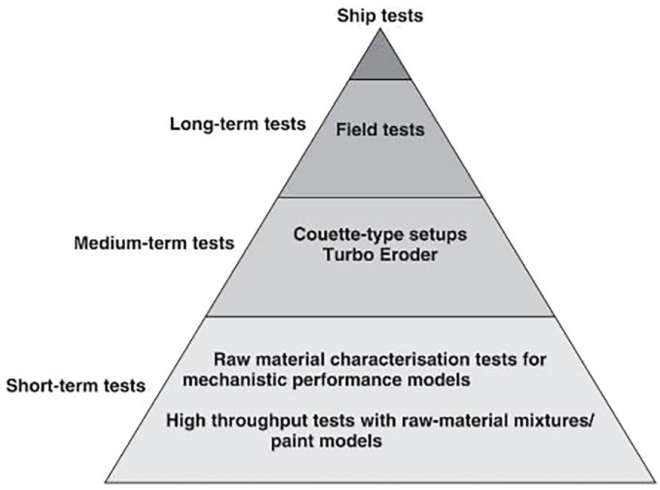

Figure 1. *The efficient antifouling coating design and optimization workflow adapted from [40]*

controlled degree of fouling. The three-month time frame in an experimental setting likely captures a mature yet actively managed fouling community, similar to the hull condition of these frequently used commercial ships.

In contrast, experimental deployments extending from six to twelve months resulted in fouling accumulation of greater complexity and biomass. These extensive fouling communities are comparable to those documented on vessels that have remained idle for prolonged periods [43,44]. During extended static conditions, hydrodynamic forces that would typically inhibit the settlement of fouling organisms are absent. This allows for the development of diverse and well-established biofouling, including macroalgae and larger invertebrates, mirroring the state of long-berthed or laid-up vessels [43].

Furthermore, it is evident from the literature that a shorter immersion period of approximately ten weeks for experimental panels corresponds to an early stage of biofouling development. This level of fouling is similar to that expected on a recreational fishing vessel subject to seasonal use [30,45]. Such vessels often experience intermittent activity with potentially extended periods of mooring during off-seasons, allowing for the initial colonisation and establishment of initiative fouling species. The ten-week exposure likely reflects this early successional stage, characterized by biofilm formation and the settlement of initial macrofouling organisms, before significant biomass or community complexity is achieved.

American Society for Testing and Materials (ASTM) released a standard [ASTM D3623-78a (2020)] that determined how these anti-fouling tests should be conducted [46]. According to this standard immersion panel area shall be a minimum of 465 cm^2. This standard was taken as a reference for the immersion tests. In addition to that, the US Navy developed a fouling grade system, Naval Ship's Technical Manual (NSTM) [47]. According to the NSTM fouling rating system, fouling accumulation was graded between 0 and 100, whilst fouling rating 0 representing the no-foul surface and fouling rating 100 denotes the most severe biofouling intensity. The NSTM report classifies fouling with the characteristics of fouler organisms, such as soft, hard or composite, while soft fouling has minimal impact, hard and composite types significantly impair hydrodynamic performance and damage coatings and machinery. Furthermore, for each rating grade, pictures of fouling conditions with the fouling grade are presented within the NSTM report.

Furthermore, by conducting antifouling coating performance tests deployed over time, a model can be used to determine extended fouling conditions on a specific surface coated with the same antifouling coating. To do that, biofouling accumulation on antifouling-coated surfaces is required to be mimicked. In the existing literature, there are two growth model configurations suitable for modelling biofouling [48]. The first is an exponential growth model, and the other is a logistic growth model. The exponential logistic growth model assumes that there is an unlimited amount of nutrition in the environment. Therefore, while an exponential growth model may hold validity in conditions where resources are unlimited, it is inadequate for accurately portraying the temporal dynamics of biofouling in marine environments, which are characterized by finite resources. This necessitates the use of more appropriate growth models. On the other hand, the logistic growth model considers exponential growth as the early-stage growth, but then takes the carrying capacity into account; therefore, an "S" shaped model is generated. Consequently, as the exponential growth model becomes unrealistic to represent biofouling accumulation over time, the logistic growth model remains the most suitable growth model representing the fouling accumulation over time.

To the best of the authors' knowledge, no study has systematically investigated the biofouling accumulation patterns and antifouling coating performance on recreational vessels constructed from GFRP using a time-dependent modelling approach. While the antifouling performance of coatings—particularly SPC—has been widely studied on commercial steel-hulled vessels, limited research has addressed how these coatings perform on GFRP hulls over time. This gap highlights a critical need for experimental studies focused on the temporal dynamics of fouling patterns on vessels with GFRP hulls, supported by robust modelling frameworks such as the logistic growth model, to better inform coating selection, maintenance strategies, and environmental impact assessments for the recreational boating sector.

2. Methodology

Methodology of this research is presented in this section, starting from the sample panels manufacturing, coating application and sample panels monitoring.

2.1. Sample Panel Manufacturing

This investigation intends to replicate real application conditions prevalent among recreational fishermen to quantitatively assess the effect of selected antifouling coating. Specifically, coating samples were applied utilizing a roller brush, a methodology widely adopted within this user group, thereby ensuring the practical relevance of the findings [49]. The experimental design was conceived to simulate the operational environment of recreational fishing vessel hulls typically navigating the Black Sea. To further enhance the reliability and replicate the in-situ performance of the antifouling coating, test panels were fabricated using the same materials, glass fiber/polyester, same lay-up configurations, and the same manufacturing techniques identical to those utilized in the construction of small marine crafts common in the region. This approach aimed to provide a realistic evaluation of the antifouling coatings' performance of a recreational fishing boat hull manufactured using GFRP.

The reference vessel for this study is a 4.95-meter recreational fishing boat as illustrated in Figure 2. To ensure the representativeness of the test specimens, the manufacturing protocol mirrored that typically employed for the construction of such marine craft.

The fabrication process commenced with the application of a protective gelcoat layer onto a prepared, smooth surface. Specifically, a dual-layer application of marine-grade gelcoat was applied via a spray gun, achieving a cumulative thickness designed to provide substantial protection against environmental degradation, including UV radiation and water ingress, as well as to offer a degree of resistance to superficial mechanical damage. In conventional boat building, this gelcoat is typically applied to the internal surface of a female mold. However, for the purposes of this study, which focused on flat panel testing, an 18 mm-thick sheet of plywood, which had been previously coated and polished to achieve a high-quality surface finish, served as the flat male mold.

Figure 2. *A typical recreational fishing vessel commonly observed in the black sea region, whose hull structure served as the reference for the design and preparation of the experimental panel samples*

Following an adequate gel time to allow for the initial curing and consolidation of the gelcoat layer, the structural laminate was constructed. This involved the sequential hand lay-up of five plies of 450 g/m² chopped strand mat glass fiber reinforcement. Each ply was carefully wetted out with polyester and consolidated to ensure thorough impregnation and minimize voids.

This fabrication process yielded test panels with a nominal overall thickness of approximately 5.0 mm. This total thickness was constituted by a 0.5 mm layer of cured gelcoat and a 4.5 mm thick GFRP laminate, resulting from the five plies of 450 g/m². This standardized sample preparation ensures that subsequent analyses accurately reflect the material properties and performance characteristics of a structure manufactured using this conventional technique.

After a 24-hour curing period, which ensured adequate solidification and stabilization of the composite material, the prepared samples were advanced to the drilling holes stage. For the purpose of secure mounting within the designated test frame, a hole was precisely drilled in each corner of every sample. Significant attention was dedicated to the drilling methodology to prevent the initiation of micro-cracks or fractures on the delicate gelcoat surface. This was achieved through a meticulous, multi-stage drilling protocol. Initially, pilot holes of a substantially smaller diameter than the final requirement were introduced. Subsequently, the drill bit diameter was incrementally enlarged in a stepwise manner until the target hole of 5 mm was attained. This progressive drilling technique was implemented to minimize stress concentrations and ensure the integrity of the sample material surrounding the hole. Geometrical characteristics of test panels are visually depicted in Figure 3 (a).

2.2. Coating Application and Frame Construction

Prior to coating application, the gelcoat surface was mechanically prepared by sanding with an 80-grit abrasive paper. This procedure was implemented to enhance the surface profile, thereby facilitating improved mechanical keying and promoting robust adhesion of the subsequent antifouling coating layer. The final appearance of the sample panels before coating application is given in Figure 3 (b).

The test panels underwent painting using a roller brush. This method was deliberately chosen due to its widespread adoption and common practice among recreational fishermen in the Black Sea region, thereby ensuring the experimental methodology closely mirrored real-world application scenarios. Therefore, the coating application was directed by the person responsible for hull paintings at a fishing port where local recreational vessels are typically serviced. In this context, the antifouling paint selected was the one most used among recreational vessels. Furthermore, the application was carried out using the roller painting method, which is a widely adopted technique among recreational boat users. Although antifouling coating's data sheet indicates that the average coating thickness typically ranges between 150-200 µm, by mimicking the real application conditions, measurements such as the thickness of the applied coating were not taken into consideration. In this study, uncoated blank specimens were assigned to the designations "B1" and "B2", and samples coated by means of a roller brush application were denoted as "R1" and "R2".

The specific antifouling coating used was a commercially available product designed for recreational vessels with wooden or GFRP hulls. The selected coating is a SPC antifouling coating that combines cuprous oxide (Cu_2O), Diuron, and N-cyclopropyl-N'-(1,1-dimethylethyl)-6-(methylthio)-1,3,5-triazine-2,4-diamine. The composition of the selected antifouling coating was obtained from the manufacturer's data sheet, which the authors have chosen not to disclose for commercial reasons. Adherence to the manufacturer's Material Data Sheet (MDS) was strictly maintained throughout the application process to ensure optimal performance characteristics and consistency. Following the initial application of the first coat, a precisely observed inter-coat interval of one hour was maintained before the second layer was applied. In accordance with the MDS specifications, no thinner was added to the coating, preserving its intended viscosity and active ingredient concentration.

Furthermore, a support structure, specifically a frame, was conceptualized and constructed to suspend experimental samples. The material of choice for this frame was Polypropylene Random Copolymer (PPRC). This selection was based on PPRC's inherent resistance to corrosion in a seawater environment, a critical factor to prevent any material degradation from influencing the experimental outcomes. To ensure the frame's submersion, a hollow pipe of PPRC with a 32 mm diameter was chosen. These pipes were precisely cut to the required dimensions and subsequently joined using a plastic welding technique. The final frame was designed with dimensions of 120x120 cm, providing ample area to accommodate the samples. For sample attachment, strategic holes were drilled into the pipes. Samples were then secured to the frame at each corner using plastic cable ties. To mitigate the possibility of contact between adjacent samples, additional diagonal tying was implemented, thereby ensuring spatial separation and preventing potential interference effects. Figure 3 (c) illustrates the final setup for the deployment tests.

Overall, a site frequently utilized for the mooring of local recreational vessels was selected to facilitate the deployment of the experimental frame. The immersion test panel apparatus was submerged at 135 cm depth from the surface, complying with the ASTM standard [ASTM D3623-78a (2020)] [46]. This location was chosen to replicate authentic environmental conditions. The frame was subsequently secured at its upper vertices to the harbor and suspended in water.

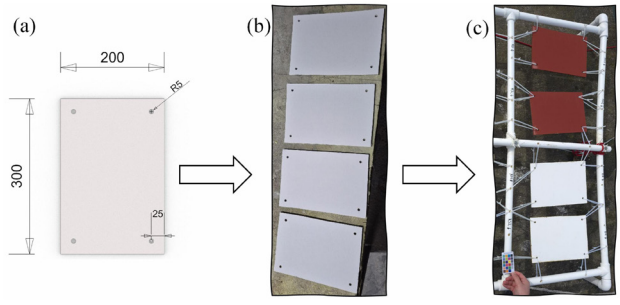

Figure 3. *Geometry of sample panels (a), the samples in their final stage prior to coating application (b), immersion test panels kit for the deployment experiment (c)*

2.3. Biofouling Monitoring and Analysis

To track the progressive accumulation of biofouling, immersed sample panels were systematically monitored at weekly intervals throughout a ten-week observation period. Recent studies have demonstrated ongoing applicability of NSTM fouling ratings. For instance, Tamburri et al. [50] conducted a research to evaluate ship-in-water cleaning and capture systems by using NSTM fouling rating in image processing to automate fouling assessment. Dinis et al. [51] developed a novel tool for ship underwater hull maintenance by using the NSTM fouling rating system. Therefore, the NSTM Fouling rating system was used to quantify fouling accumulation over time in this research. To do that, instructions with the descriptions were considered from NSTM [46]; therefore, notes were taken for each week and the panel's biofouling condition. As a result, fouling ratings of each panel over time were attended. Table 1 gives

the description of the fouling patterns and attributed fouling ratings adapted from NSTM [47].

Following that, attributed NSTM fouling ratings were fitted into logistic growth model using MATLAB software's Curve fitting tool. To do that, a logistic growth model was developed based on the logistic growth models suggested by Sarkar [48] and Uzun et al. [52]. The logistic growth model equation representing biofouling accumulation over time is given in Equation 1.

$$FR_{NSTM} = \frac{P-p}{1+(exp^{b-ct})} + \frac{d}{1+(exp^{f-gt})} + \frac{m}{1+(exp^{n-ot})} \quad (1)$$

Where FR_{NSTM} is the fouling ratings according to NSTM standards, P, p, b, c, d, f, g, m, n, and o are logistic growth model constants, and t is the sum of immersion time in days. As a result, fouling ratings and relevant models of the panels immersed over 10 weeks are presented in plots. Plots include the specific panel codes with the logistic growth models. So that the natural growth of the fouling over immersed panels can be predicted using Equation 1 with the given constants. Concurrent with the weekly acquisition of sample images, environmental variables, such as water temperature and salinity, were systematically monitored and recorded.

Schultz [5] investigated the coating roughness and the impacts of biofouling on ship resistance and powering. In this study, a table was demonstrated correlating the NSTM fouling ratings, the equivalent sand roughness heights (k_s) and average coating roughness (Rt_{50}). The range of representative fouling conditions, corresponding NSTM fouling ratings with equivalent k_s and Rt_{50} values are given in Table 2.

Biofouling monitoring and analysis step was finally concluded by generating two further equations with the aim of converting NSTM fouling ratings to industrially accepted roughness scales k_s and Rt_{50} values.

3. Results and Discussion

Biofouling accumulation over time was periodically observed in the natural marine environment for the recreational vessels. To do that, panels representing hull material were coated with a commercially available antifouling coating and checked periodically with the aim of observing biofouling over time. The material used in the immersion test panels was selected to represent the recreational vessel's hull material. At the same time, weekly seawater temperature and salinity with the atmospheric temperatures measured to check for any anomalies in seawater. Recorded seawater temperatures, salinity and weather temperatures are presented in Table 3.

Analysis of the data presented in Table 3 demonstrates that, despite minor temporal fluctuations, a consistent long-term upward trend is observed for both weather and seawater temperatures. Conversely, salinity levels were observed to fluctuate within a range of 18-20.5%. While such a variation in salinity was not anticipated, this deviation can be attributed to the lack of control over the environmental

Table 1. *NSTM fouling ratings, adapted from [47]*

Fouling ratings	Description of the fouling patterns
0	A clean, foul-free surface; red and/or black AF coating or a bare metal surface.
10	Light shades of red and green (incipient slime). Bare metal and coated surfaces are visible beneath the fouling.
20	Slime as dark green patches with yellow- or brown-colored areas (advanced slime). Bare metal and coated surfaces may be obscured by the fouling.
30	Grass as filaments up to 3 inches (76 mm) in length, projections up to 1/4 inch (6.4 mm) in height; or a flat network of filaments, green, yellow, or brown in color; or soft non calcareous fouling such as sea cucumbers, sea grapes, or sea squirts projecting up to 1/4 inch (6.4 mm) in height. The fouling can not be easily wiped off by hand.
40	Calcareous fouling in the form of tubeworms less than ¼ inch in diameter or height.
50	Calcareous fouling in the form of barnacles less than ¼ inch in diameter or height.
60	Combination of tubeworms and barnacles, less than ¼ inch (6.4 mm) in diameter or height.
70	Combination of tubeworms and barnacles, greater than ¼ inch in diameter or height.
80	Tubeworms closely packed together and growing upright away from surface. Barnacles growing one on top of another, ¼ inch or less in height. Calcareous shells appear clean or white in color.
90	Dense growth of tubeworms with barnacles, ¼ inch or greater in height; Calcareous shells brown in color (oysters and mussels); or with slime or grass overlay.
100	All forms of fouling present, soft and hard, particularly soft sedentary animals without calcareous covering (tunicates) growing over various forms of hard growth.
NSTM: Naval Ship's Technical Manual	

conditions prevalent within the port during the immersion tests. However, since recreational vessels spend their idle time in the ports, this condition represents a realistic perspective in the biofouling immersion tests. Building on these environmental observations, the subsequent sections present the fouling growth results and analyse them using a logistic growth model.

3.1. Fouling Growth Analysis

This study specifically aimed to characterise the early stages of biofouling development. Consequently, the test panels were retrieved from the Black Sea after a 10-week immersion period. To do that, immersed panels were checked regularly to distinguish fouling patterns over time using the descriptions from Table 1. From the immersion day to the final day of the immersion tests, panels were periodically observed, notes taken, and the fouling ratings given with the descriptions from Table 1 were attended. Within this point, it is important to state that semi-ratings (such as 5,15 and 25) were also considered when the fouling patterns are not clear; therefore, the authors could not fit the ratings in an NSTM fouling rating grade. Attended NSTM fouling ratings are given in Table 4.

It can be seen from Table 4 that coated and uncoated surfaces show differences in terms of fouling ratings. Moreover, while uncoated surfaces face advanced slime accumulation (NSTM fouling rating of 20) within the first month (Week 4), antifouling coatings prove high effectiveness in combating.

When uncoated panels (B1 and B2) are examined in detail, fouling patterns show similarities as expected. However, uncoated surfaces fail to prevent biofouling accumulation for both panels. In other words, both panels show indications of incipient slime accumulation (fouling rating 10) with the first 2 weeks, and yet in the 4th week, advanced slime accumulation (fouling rating 20) is observed. Within the 10-week immersion period, grass filaments became visible as the severest fouling condition over B2 and therefore the maximum fouling rating reached is 30. Another important point to notice is that although general trends indicate increases in the severity of biofouling—and consequently higher NSTM fouling ratings—the B2 panel shows a slight decline in NSTM ratings. More specifically, after week 8 of the B2 panel, there is a decline in the NSTM fouling ratings of B2. Although the reason behind this is unclear, wave patterns in the immersion site or the organisms that are fed

Table 2. *Fouling condition descriptions, equivalent NSTM fouling ratings, equivalent sand roughness heights (μm) and average coating roughness (μm), adapted from Schultz [5]*

Description of fouling conditions	NSTM fouling rating	k_s (μm)	Rt_{50} (μm)
Hydrodynamically smooth surfaces	0	0	0
Typical as applied AF coating	0	30	30
Deteriorated coating or light slime	10-20	100	100
Heavy slime	30	300	300
Small calcareous fouling or weed	40-60	1000	1000
Medium calcareous fouling	70-80	3000	3000
Heavy calcareous fouling	90-100	10000	10000
NSTM: Naval Ship's Technical Manual			

Table 3. *Environmental variables during the 10-week immersion period*

Immersion duration (weeks)	Seawater temp. (°C)	Salinity (%)	Weather temp. (°C)	Sky condition
0	10	20	13	Partly cloudy
1	13	19	23	Partly cloudy
2	9	20	6	Rainy
3	13	19.5	18	Mostly cloudy
4	13	18.5	17	Rainy
5	11	20.5	9	Mostly cloudy
6	12	19	14	Mostly cloudy
7	14	19.5	16	Cloudy
8	12	19.5	12	Mostly cloudy
9	18	18	27	Sunny
10	16.5	20	24	Sunny

by the fouler organisms can cause this problem, similar to the incident reported by Özyurt [53]. In that study, a similar condition was observed and reported. A pipefish (Syngnathus typhle) was naturally feeding on fouling organisms, which led to a noticeable decrease in the NSTM ratings.

Moreover, fouling ratings for the coated panels R1 and R2 show similarities. Whilst incipient slime accumulation becomes visible starting from the 4th week, the maximum fouling rating that is reached for the coated panels R1 and R2 is 20, after a 10-week immersion period. Thus, coated panels R1 and R2 show greater success at preventing biofouling in comparison to the uncoated panels B1 and B2. In detail, whilst the second week becomes the initial stage of the incipient slime accumulation on B1 and B2, it is the fourth week that the incipient slime becomes visible for the coated R1 and R2 panels. Furthermore, during the 10-week of immersion time, while the uncoated panels B1 and B2 show the highest fouling ratings of 30 in the sixth week, the highest fouling rating for the coated R1 and R2 is the fouling rating 20 after a ten-week immersion period.

Within this point, it is important to note that while conducting antifouling tests in the natural sea environment provides realistic insights, they are limited by lack of control. Additionally, seasonal and geographical changes result in significant changes in biofouling accumulation due to the factors affecting biofouling growth, including seawater temperature, salinity, pH, nutrient availability, and immersion depth. However, considering the accuracy of the antifouling tests presented in Figure 1, validation through full-scale testing on an actual vessel is ideally required, but such an undertaking is often not feasible due to high costs. Therefore, the most feasible method to test antifouling coatings is the immersion tests. Further details of the aspects among varying antifouling ageing tests are investigated in the research conducted by Hellio and Yebra [27]. The resultant final condition of the panels is presented in Figure 4, providing a clearer representation of biofouling accumulation at the end of the 10th week.

Figure 4 illustrates the overall performance of antifouling coatings on GFRP materials. It is visually apparent that while coated surfaces are successful at preventing biofouling accumulation, uncoated surfaces fail to prevent biofouling accumulation after a 10-week immersion time. After the fouling ratings were attended for each test panel, a Logistic growth model was fitted into the generated data.

3.2. Logistic Growth Model Fitting

After generating a data set representing biofouling growth over time, a logistic growth model was fitted into the data set with the aim of predicting certain NSTM fouling rating at a given immersion period; therefore, further calculations can be conducted for the recreational vessels operating under a certain operational profile. Fitted logistic growth models using the data presented in Table 4 and Equation 1 are plotted and presented in Figure 5.

Figure 5 demonstrates fouling accumulation trends of two uncoated (B1 and B2) and two coated (R1 and R2) panels over approximately 70 days of immersion, modelled utilizing a logistic growth model, Equation 1, to describe NSTM fouling ratings. Additionally, logistic growth model's constant values with the R-squared values (RSQ), adjusted RSQ, sum of squared error values and root mean squared error values are presented in Figure 5. Overall, results demonstrate that the logistic growth model exhibits a strong correlation with the Immersion Field test data, particularly for B1, R1 and R2, which shows excellent correlations with the high RSQ values. Additionally, although B2 shows a lower RSQ value, the correlation is sufficient, supporting the suitability of the model for stimulating biofouling growth over time and provides confidence in predicting the NSTM fouling ratings for the given immersion time.

Lower RSQ value for B2 can be attributed to the fouling removal, as discussed in Section 3.1. Since the logistic growth model considers population growth and neglects the decrease in population dynamics, as demonstrated by Sarkar [48], an imbalance between observed data and model predictions is expected when the fouling is actively removed.

Figure 5 also highlights the effectiveness of antifouling coatings. While an uncoated recreational vessel's GFRP hull is only capable of preventing advanced slime accumulation up to 30-35 days, coating application can delay advanced slime accumulation approximately 35 days, which is visible from

Table 4. *Attended NSTM fouling ratings over a 10-week immersion period*

Weeks	NSTM ratings			
	B1	B2	R1	R2
0	0	0	0	0
1	5	5	5	5
2	10	10	5	5
3	10	10	5	5
4	15	15	10	5
5	20	20	10	10
6	25	30	10	10
7	25	30	10	10
8	25	30	10	10
9	25	25	15	15
10	25	25	20	20

NSTM: Naval Ship's Technical Manual

both test panels and their replicas. Furthermore, while an uncoated GFRP hull cannot resist grass filaments appearing on its surface between 35-40 days, coating application can delay grass filaments appearing on the recreational vessel's hull more than nearly 70 days.

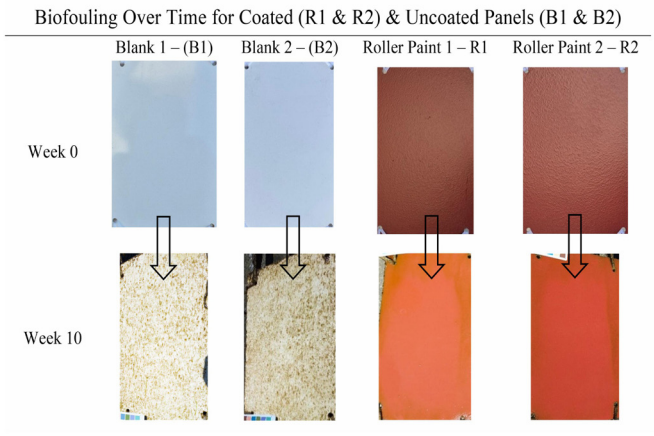

Figure 4. *State of panels blank 1 (B1), blank 2 (B2), roller paint 1 (R1), roller paint 2 (R2) after 70 days (week 10) of immersion*

Overall, fitted curves illustrated in Figure 5 make a prediction of the NSTM fouling ratings. By using Equation 1 and the given constants within Figure 5 for each immersion test panel (B1, B2, R1, and R2), it is possible to predict the fouling condition of any surface for the given immersion time.

Finally, in addition to the curves fitted into the logistic growth model, a further correlation between roughness scale, in terms of equivalent sand roughness heights (k_s), average coating roughness (Rt_{50}), and NSTM fouling ratings is plotted and presented in Figure 6.

Figure 6 illustrates the correlations between NSTM fouling ratings, equivalent sand roughness heights and Average Coating Roughness in μm. The equations given in Figure 6 are particularly important for those willing to investigate the impacts of biofouling on a recreational boat made of GFRP with coated and/or uncoated hull conditions, considering the operational profile of the vessels.

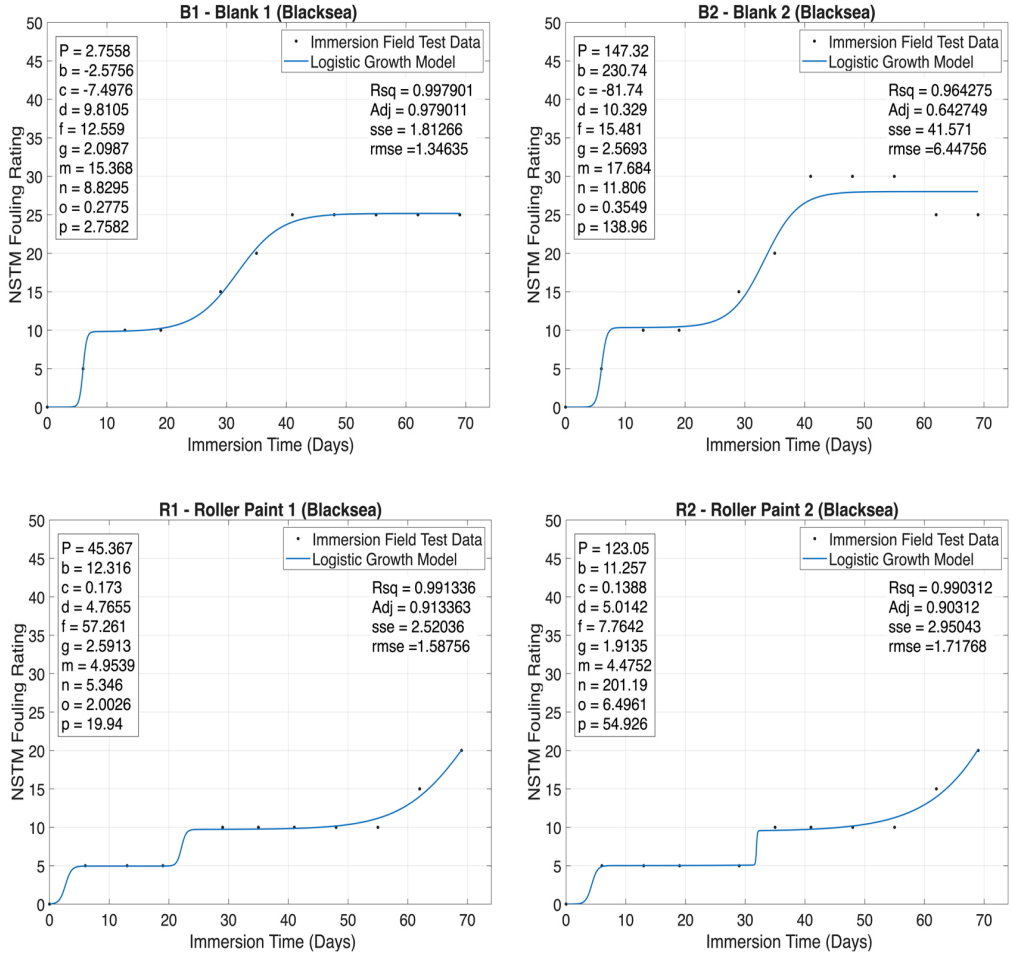

Figure 5. *Logistic growth fitting for the NSTM fouling ratings for the surfaces deployed*

NSTM: Naval Ship's Technical Manual

4. Conclusion

Biofouling over a coated and uncoated GFRP material showed significant differences in terms of initial fouling growth. This growth was quantified using the NSTM fouling rating system to be converted into varying roughness scales, including equivalent sand roughness heights (k_s) and average coating roughness (Rt_{50}). Subsequently, the obtained NSTM fouling rating data were fitted to a logistic growth model to characterize the natural progression of biofouling over time. Utilizing the logistic growth parameters presented in Figure 5 and Equation 1, the temporal evolution of NSTM fouling ratings can be estimated. Following the model fitting, additional correlations were established between the NSTM fouling ratings, k_s, and Rt_{50}. Based on these relationships, two predictive equations—depicted in Figure 6—were formulated to estimate k_s and Rt_{50} values as a function of the NSTM fouling ratings. Collectively, these equations, in conjunction with Equation 1, enable the prediction of roughness parameters over a specified fouling period. As a result, antifouling coating immersion test results showed that coating GFRP material with an SPC coating becomes highly efficient in terms of preventing fouling growth over time. More specifically, while coating a recreational boat with a GFRP hull can prevent advanced slime accumulation for 60 to 70 days, uncoated hulls are subjected to advanced slime accumulation in nearly 30-40 days. With this in mind, biofouling has been shown to increase effective power requirements by up to 24%, which in turn raises fuel consumption and CO_2 emissions for fishing vessels with steel hulls over a fishing season, as reported by Ozyurt et al. [30]. Considering the total operational profile of the recreational vessels, this time gap can make a significant contribution to the overall efficiency of the vessel, leading to reduced fuel consumption, fuel costs and CO_2 emissions.

5. Future Work

Although this study does not include quantitative data on fuel consumption or emissions reductions, the observed reduction in fouling with SPC coatings suggests a potential for improved operational efficiency and reduced environmental impact. These implications align with trends reported in previous literature [5-8] and warrant further investigation through dedicated empirical studies. This research may lead researchers to further investigate the potential benefits of GFRP materials constructed recreational fishing boats concerning biofouling. This can be helpful for the decision-maker authorities adopting new regulations for the recreational fishing vessels, which can particularly be preserved both marine ecosystem and air pollution due to toxic material release into the marine environment from SPC coatings and the added emissions released caused by increased fuel consumption. This data can be further extrapolated to investigate the impacts of the recreational fishing boats concerning the GFCM area and globally. To gain a more complete understanding of long-term biofouling dynamics, subsequent research should incorporate extended immersion periods, ranging from six to twelve months, to mimic vessels remaining idle for protracted durations. In addition, the scope of the research can be broadened by conducting similar field tests in different marine environments, such as the Baltic Sea, the Caspian Sea or the Mediterranean Sea. A further study would facilitate a direct comparison of biofouling characteristics over typical steel and GFRP constructed hulls. In addition, a life cycle analysis can be conducted considering a recreational vessel's lifespan between steel-hulled and GFRP-hulled vessels. In parallel, a comprehensive investigation into the impacts of antifouling coatings on the environment can be investigated to underline how marine organisms and biodiversity are affected.

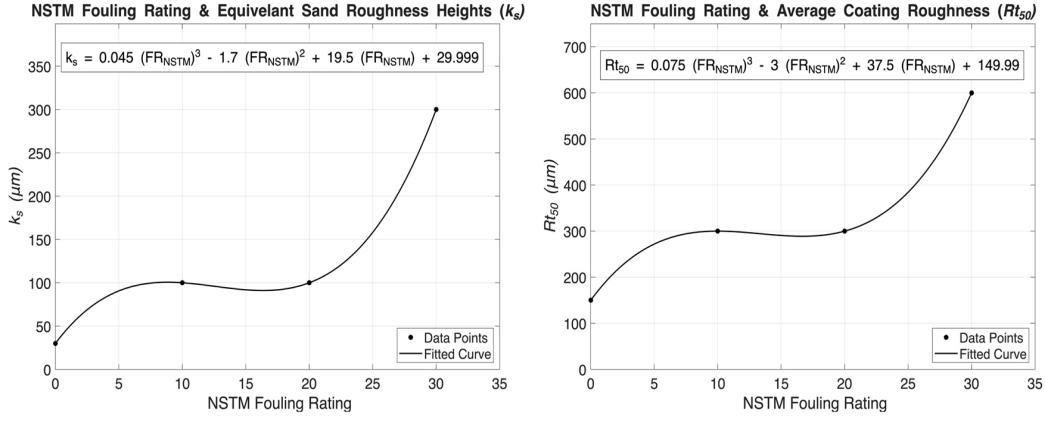

Figure 6. *NSTM fouling ratings (FR_{NSTM}) against equivalent sand roughness heights (k_s) correlations (a) and average coating roughness (Rt_{50}) correlations (b)*

NSTM: Naval Ship's Technical Manual

Footnotes

Authorship Contributions

Concept design: R. Özyurt, and M. Cihan, Data Collection or Processing: R. Özyurt, and M. Cihan, Analysis or Interpretation: R. Özyurt, Literature Review: R. Özyurt, and M. Cihan, Writing, Reviewing and Editing: R. Özyurt, and M. Cihan.

Funding: The authors did not receive any financial support for the research, authorship and/or publication of this article.

References

[1] D. Uzun, R. Ozyurt, Y. K. Demirel, and O. Turan, "Does the barnacle settlement pattern affect ship resistance and powering?," *Applied Ocean Research*, vol. 95, 102020, Feb 2020.

[2] J. Bannister, M. Sievers, F. Bush, and N. Bloecher, "Biofouling in marine aquaculture: a review of recent research and developments," *The Journal of Bioadhesion and Biofilm Research*, vol. 35, pp. 631-648, Jul 2019.

[3] A. Farkas, N. Degiuli, I. Martić, M. Barbarić, and Z. Guzović, "The impact of biofilm on marine current turbine performance," *Renewable Energy*, vol. 190, pp. 584-595, May 2022.

[4] M. Maduka, F. Schoefs, K. Thiagarajan, and A. Bates, "Hydrodynamic effects of biofouling-induced surface roughness – Review and research gaps for shallow water offshore wind energy structures," *Ocean Engineering,* vol. 272, 113798, Mar 2023.

[5] M. P. Schultz, "Effects of coating roughness and biofouling on ship resistance and powering," *The Journal of Bioadhesion and Biofilm Research*, vol. 23, pp. 331-341, Oct 2007.

[6] M. P. Schultz, J. A. Bendick, E. R. Holm, and W. M. Hertel, "Economic impact of biofouling on a naval surface ship," *The Journal of Bioadhesion and Biofilm Research*, vol. 27, pp. 87-98, Jan 2011.

[7] A. Farkas, N. Degiuli, I. Martić, and M. Vujanović, "Greenhouse gas emissions reduction potential by using antifouling coatings in a maritime transport industry," *Journal of Cleaner Production,* vol. 295, 126428, May 2021.

[8] IMO, "Guidelines for the control and management of ships' biofouling to minimize the transfer of invasive aquatic species," 2011.

[9] S. Cao, J. Wang, H. Chen, and D. Chen, "Progress of marine biofouling and antifouling technologies," *Chinese Science Bulletin,* vol. 56, pp. 598-612, Mar. 2011.

[10] H. Jin, L. Tian, W. Bing, J. Zhao, and L. Ren, "Bioinspired marine antifouling coatings: Status, prospects, and future," *Progress in Materials Science,* vol. 124, 100889, Feb 2022.

[11] L. Chen, et al. "Biomimetic surface coatings for marine antifouling: Natural antifoulants, synthetic polymers and surface microtopography," *Science of The Total Environment,* vol. 766, 144469, Apr 2021.

[12] Z. Li, et al. "Bioinspired marine antifouling coatings: Antifouling mechanisms, design strategies and application feasibility studies," *European Polymer Journal,* vol. 190, 111997, May 2023.

[13] M. Legg, M. K. Yücel, I. Garcia De Carellan, V. Kappatos, C. Selcuk, and T. H. Gan, "Acoustic methods for biofouling control: A review," *Ocean Engineering*, vol. 103, pp. 237-247, Jul 2015.

[14] M. Rahmoune and M. Latour, "Application of mechanical waves induced by piezofilms to marine fouling protection of oceanographic sensors," *Smart Materials and Structures,* vol. 4, pp. 195, 1995.

[15] E. Ryan, S. Turkmen, and S. Benson, "An Investigation into the application and practical use of (UV) ultraviolet light technology for marine antifouling," *Ocean Engineering*, vol. 216, Nov 2020.

[16] F. W. Y. Myan, "*The influence of physical attributes of surface topographies in relation to marine biofouling*," The University of Nottingham Ningbo China, 2016. Accessed: Apr 04, 2019. [Online]. Available: http://eprints.nottingham.ac.uk/38837/1/The Influence of Physical Attributes of Surface Topographies in Relation to Marine Biofouling.pdf

[17] M. J. Romeu, and F. Mergulhão, "Development of antifouling strategies for marine applications," *Microorganisms,* vol. 11, pp. 1568, Jun 2023.

[18] B. Dahlbäck, H. Blanck, and M. Nydén, "The challenge to find new sustainable antifouling approaches for shipping," *Coastal Marine Science*, vol. 34, pp. 212-215, 2010.

[19] M. Lagerström, E. Ytreberg, A. K. E. Wiklund, and L. Granhag, "Antifouling paints leach copper in excess – study of metal release rates and efficacy along a salinity gradient," *Water Research,* vol. 186, 116383, Nov 2020.

[20] M. Candries, M. Atlar, and C. D. Anderson, "Estimating the impact of new-generation antifoulings on ship performance: The presence of slime," *Journal of Marine Engineering & Technology,* vol. 2, pp. 13-22, 2003.

[21] D. M. Yebra, S. Kiil, and K. Dam-Johansen, "Antifouling technology—past, present and future steps towards efficient and environmentally friendly antifouling coatings," *Progress in Organic Coatings,* vol. 50, pp. 75-104, Jul 2004.

[22] L. D. Chambers, K. R. Stokes, F. C. Walsh, and R. J. K. Wood, "Modern approaches to marine antifouling coatings," *Surface and Coatings Technology,* vol. 201, pp. 3642-3652, Dec 2006.

[23] P. Buskens, M. Wouters, C. Rentrop, and Z. Vroon, "A brief review of environmentally benign antifouling and foul-release coatings for marine applications," *Journal of Coatings Technology and Research,* vol. 10, pp. 29-36, 2013.

[24] P. Hu, Q. Xie, C. Ma, and G. Zhang, "Silicone-based fouling-release coatings for marine antifouling," *Langmuir Journal*, vol. 36, pp. 2170-2183, Mar 2020.

[25] I. A. Yeginbayeva, M. Atlar, S. Turkmen, and H. Chen, "Effects of 'in-service' conditions–mimicked hull roughness ranges and biofilms–on the surface and the hydrodynamic characteristics of foul-release type coatings," *The Journal of Bioadhesion and Biofilm Research,* vol. 36, pp. 1074-1089, Dec 2020.

[26] C. Anderson, M. Atlar, M. Callow, M. Candries, A. Milne, and R. Townsin, "The development of foul-release coatings for seagoing vessels," *Proceedings of the Institute of Marine Engineering, Science, and Technology. Part B, Journal of marine design and operation,* vol. 4, pp. 11-23, Jan 2003.

[27] C. Hellio, and D. Yebra, *Advances in Marine Antifouling Coatings and Technologies*. Cambridge: Woodhead Publishing Limited, 2009.

[28] A. K. Leonardi, and C. K. Ober, "Polymer-based marine antifouling and fouling release surfaces: Strategies for synthesis and modification," *Annual Review of Chemical and Biomolecular Engineering,* vol. 10, pp. 241-264, Jun 2019.

[29] Z. Dai, et al. "A novel marine antifouling coating based on a self-polishing zinc-polyurethane copolymer," *Journal of Coatings Technology and Research,* vol. 18, pp. 1333-1343, Sep. 2021.

[30] R. Ozyurt, D. Uzun, Y. Terzi, S. Şaffak, M. Atlar, and O. Turan, "A simple antifouling coating selection exhibits notable benefits for industrial fishing vessels," *Ocean Engineering*, vol. 288, 115955, Nov 2023.

[31] N. X. Thai, et al. "Assessment of marine antifouling property of fluoropolymer nanocomposite coating on steel substrate - A preliminary assay in laboratory," *Vietnam Journal of Chemistry,* vol. 61, pp. 28-35, Jun 2023.

[32] P. P. Falara, N. D. Papadopoulos, and P. Vourna, "Microstructure and performance of antibiofouling coatings on high-strength steel substrates immersed in the marine environment," *Micro*, vol. 2, pp. 277-294, May 2022.

[33] J. Zhao, et al. "Controllable release of Cu ions contributes to the enhanced environmentally-friendly performance of antifouling Cu-bearing stainless steel coating prepared using high-velocity air fuel," *Surface and Coatings Technology,* vol. 481, 130629, Apr 2024,

[34] W. Zhou, et al. "Nanostructured antifouling coatings for galvanized steel food storage and container surfaces to enhance hygiene and corrosion resistance against bacterial, fungal, and mud contamination," *Journal of Food Engineering,* vol. 363, 111784, Feb 2024.

[35] S. Daloğlu, N. Çöpoğlu, O. Karaahmet, and B. Çiçek, "Antifouling performance of TiO2-based SiO2–Na2O–K2O glass-ceramic coatings in marine environments," *Materials Chemistry and Physics,* vol. 312, 128649, Jan 2024.

[36] R. K. Suleiman, T. A. Saleh, O. C. S. Al Hamouz, M. B. Ibrahim, A. A. Sorour, and B. El Ali, "Corrosion and fouling protection performance of biocide-embedded hybrid organosiloxane coatings on mild steel in a saline medium," *Surface and Coatings Technology,* vol. 324, pp. 526-535, Sep 2017.

[37] K. R. C. Soma Raju, A. Gautam, R. Patra, K. Srinivasa Rao, K. V. Gobi, and R. Subasri, "Bioinspired strategies for corrosion protection and antifouling coatings," *Novel Anti-Corrosion and Anti-Fouling Coatings and Thin Films,* pp. 251-285, Aug 2024.

[38] M. H. A. Kadir, M. A. Hashim, U. R. Hashim, and A. Jumahat, "Anti-fouling behaviors of polyethersulfone – coated glass fibre reinforced polymer composite," *International Journal of Sustainable Construction Engineering and Technology*, vol. 15, pp. 304-314, Dec 2024.

[39] R. V. Subramanian, and R. S. Williams, "Glass-reinforced composites of antifouling organotin epoxy polymers," *Journal of Applied Polymer Science,* vol. 26, pp. 1681-1688, May 1981.

[40] A. Sánchez, and D. M. Yebra, "Ageing tests and long-term performance of marine antifouling coatings," in *Advances in Marine Antifouling Coatings and Technologies*, *Woodhead Publishing Series in Metals and Surface Engineering,* pp. 393-421, 2009.

[41] A. D. M. Coutts and M. D. Taylor, "A preliminary investigation of biosecurity risks associated with biofouling on merchant vessels in New Zealand," *New Zealand Journal of Marine and Freshwater Research,* vol. 38, pp. 215-229, 2004.

[42] I. C. Davidson, C. W. Brown, M. D. Sytsma, and G. M. Ruiz, "The role of containerships as transfer mechanisms of marine biofouling species," *The Journal of Bioadhesion and Biofilm Research*, vol. 25, pp. 645-655, Oct 2009.

[43] G. A. Hopkins, B. M. Forrest, and A. D. M. Coutts, "The effectiveness of rotating brush devices for management of vessel hull fouling.," *The Journal of Bioadhesion and Biofilm Research*, vol. 26, pp. 555-566, 2010.

[44] I. C. Davidson, L. D. McCann, M. D. Sytsma, and G. M. Ruiz, "Interrupting a multi-species bioinvasion vector: The efficacy of in-water cleaning for removing biofouling on obsolete vessels," *Marine Pollution Bulletin,* vol. 56, pp. 1538-1544, Sep 2008.

[45] P. Rossini, L. Napolano, and G. Matteucci, "Biotoxicity and life cycle assessment of two commercial antifouling coatings in marine systems," *Chemosphere*, vol. 237, 124475, Dec 2019.

[46] ASTM, "D3623 − 78a (Reapproved 2012) Standard test method for testing antifouling panels in shallow submergence," 2012.

[47] NSTM, "Naval ships' technical manual," Washington D.C, 2002. Accessed: Oct. 02, 2018. [Online]. Available: https://maritime.org/doc/nstm/ch081.pdf

[48] S. Sarkar, "Ecology," Metaphysics Research Lab, Stanford University (Winter 2016 Edition), 2005. Accessed: Feb 08, 2022. [Online]. Available: https://plato.stanford.edu/archives/win2016/entries/ecology/

[49] R. Ozyurt, D. Uzun, M. Atlar, and O. Turan, "Biofouling Awareness and Antifouling Practices among Fishing Vessels: A Questionnaire Survey Assessment," in *5th Global Maritime Congress (GMC'24)*, İstanbul: www.globalmaritimecongress.org, May 2024, p. 550. [Online]. Available: www.globalmaritimecongress.org

[50] M. N. Tamburri, et al. "In-water cleaning and capture to remove ship biofouling: an initial evaluation of efficacy and environmental safety," *Frontiers in Marine Science,* vol. 7, 536665, Jun 2020.

[51] D. R. Oliveira, M. Lagerström, L. Granhag, S. Werner, A. I. Larsson, and E. Ytreberg, "A novel tool for cost and emission reduction related to ship underwater hull maintenance," *Journal of Cleaner Production,* vol. 356, 131882, Jul 2022.

[52] D. Uzun, Y. K. Demirel, A. Coraddu, and O. Turan, "Time-dependent biofouling growth model for predicting the effects of biofouling on ship resistance and powering," *Ocean Engineering*, vol. 191, 106432, Nov 2019.

[53] R. Özyurt, "A decision support system for the selection of most appropriate antifouling coatings for fishing vessels operating in the Mediterranean and the Black Sea," University of Strathclyde: Glasgow, 2022.